

Preparation and characterization of the electrodeposited Zn-Cr-Fe ternary alloys

ISMAIL HAKKI KARAHAN

Department of Physics, Faculty of Art and Science, Kilis 7 Aralık University, Kilis/Turkey

Ternary Zn-Fe-Cr alloys were electrodeposited under potentiostatic conditions; surface morphology and corrosion properties were investigated and contrasted with the characteristics of Zn-Fe electrodeposits. The results indicated that crystallographic structures of Zn-Cr-Fe deposits with Cr content 1 to 2 at.% have the same structure as Zn-Fe alloy. It is observed that Zn-Co-Ni alloy electrodeposition is anomalous type. The polarization measurement results indicated that the Zn-Cr-Fe alloy coatings more protective than Zn-Fe coating.

(Received November 3, 2008; accepted November 27, 2008)

Keywords: Alloys, Thin films, Chemical synthesis, X-ray diffraction, Electron microscopy

1. Introduction

Electrodeposited zinc has been used extensively in automotive and other industrial sectors as a protective coating for large quantities of steel wires, strips, sheets, tubes and other fabricated ferrous metal parts. Zinc deposits offer good protection and decorative appeal at low cost. The development of alloy deposits is of great interest mainly from the point of view of providing an economic alternative to thermally produced alloys [1,2]. The use of zinc alloys provides several advantages. Electrochemically, alloys have different corrosion potentials from their alloying elements. Alloys of zinc, for example, can be designed to maintain anodic protection to steel, but remain less electrochemically active than pure zinc. Thus, a zinc alloy coating can still be sacrificial to steel components, but corrodes much more slowly than zinc when exposed to a corrosive environment [3]. Zinc-alloy electrodeposited coatings and especially can those containing one of the 'iron group metals' (e.g. iron, nickel and cobalt) have found important end-uses in various industrial sectors. In particular, Zn-Fe electrodeposit is promising alternatives to pure Zn. Electrodeposited Fe-Zn alloy has been widely studied [4-8]. Chromium alloy deposits have gained great importance in recent years because of their considerable resistance to wear, abrasion and hardness as well as corrosion [9-13]. Much interest

has been shown, in the past five decades, in the application of Fe-Cr alloys for their attractive physical properties. Fe-Cr alloys exhibit many desirable properties such as corrosion resistance, high strength and hardness and low rate of oxidation and retention of strength at elevated temperature. As a kind of important surface protection material, Fe-Cr alloy films have been extensively applied in various industrial fields. Therefore, Fe-Cr alloy films obtained by electrodeposition method have been the subjects of investigation by a number of researchers [14-16]. Therefore, it was felt that it would be interesting to collect the properties of Zn-Fe and Fe-Cr alloys in one alloy via the electrodeposition of Zn-Fe-Cr ternary alloy.

The aim of the present work was to study corrosion behaviour of Zn-Cr-Fe alloy coatings from 1 to 19 at.% of Fe, as well as the alteration of the composition and structure of coatings caused by bath composition.

2. Experimental

Zn-Fe and Zn-Cr-Fe alloys have been electrodeposited with an approximate thickness of 2 μm on aluminium foils and AISI 4140 steel disks from chloride baths at room temperature. The chemical composition of AISI 4140 steel is given in Table 1.

Table 1. Chemical composition of AISI 4140 low alloy steel (%)

Element	C	Mn	Si	Cr	Ni	Mo	V	S	Cu	P
Wt.%	0.36	0.80	0.005	0.914	0.30	0.85	0.075	0.07	0.143	0.034

The working electrodes were aluminium foils used for XRD and AAS measurements and AISI 4140 steel disks used for corrosion. All these electrolytes were prepared from Merck pro-analysis grade chemicals using double-distilled water and consisted of ZnCl_2 67.5 gl^{-1} ,

$\text{CrCl}_3 \cdot 6\text{H}_2\text{O}$ 159 gl^{-1} , $\text{N}_2\text{HCH}_2\text{COOH}$ 200 gl^{-1} , H_3BO_3 31.5 gl^{-1} , NH_4Cl 95.4 gl^{-1} , FeCl_3 8.05, 16.1, 32.2, 80.5 for the Zn-Cr-Fe alloys and ZnCl_2 67.5 gl^{-1} , $\text{N}_2\text{HCH}_2\text{COOH}$ 200 gl^{-1} , H_3BO_3 31.5 gl^{-1} , NH_4Cl 95.4 gl^{-1} , FeCl_3 16.1 gl^{-1} for Zn-Fe alloy. The pH was adjusted by addition of an

aqueous HCl solution until a value of 3.5 ± 0.05 was reached. The plating time was 10 min, after which the cathode was withdrawn, washed with distilled water and dried.

Before electrodeposition, aluminium foils were mechanically polished with silicon carbide emery paper, degreased in 1 M NaOH with surfactant at 70 °C during 5 min and finally rinsed with the twice distilled water (18 MΩ cm) and dried in air. Counter electrode was a Pt electrode, for the polarization and the corrosion measurements. The reference electrode used in all experiments was a saturated calomel electrode (SCE). All the potentials are referred against SCE.

The corrosive behaviours of the electrodeposited specimens were analyzed in 3 wt.% NaCl aqueous solution at room temperature in a Pyrex glass cell. The corrosion behaviours of the samples were investigated by a potentiodynamic polarization technique. Polarization and cyclic voltammetry measurements were performed with an electrochemical analyzer/workstation (Model 1100, CH Instruments, USA) with a three-electrode configuration. The exposed area of the specimens was about 1 cm². The specimens were covered with a cold setting resin and immersed into the solution until a steady open circuit potential (ocp) is reached. After equilibrium, the polarization was started at a rate of 10 mV/sn.

A Rigaku diffractometer was used to analyze the crystallographic structure of alloys. The X-ray diffractometer was operated at 30 kV and 30 mA with CuK α radiation. The film composition was determined via a Perkin-Elmer atomic absorption spectrophotometer (AAS) after dissolving the deposits in concentrated hydrochloric acid and diluting the solution with distilled water to 100 ml. The results obtained by atomic absorption spectrophotometer were shown in Table 2. The error bars for the elemental compositions in table 2 is $\pm 0.1\%$. The morphologies of the deposits were analyzed by scanning electron microscopy (SEM).

Table 2. Composition of deposits.

% at electrolyte	% at deposit		
	Zn	Cr	Fe
3.4	98	1	1
6.6	95	1	4
12.4	91	2	7
26.2	80	2	18
3.4	98	0	2

3. Results and discussion

Zn-Cr-Fe alloys were electrodeposited from the electrolyte containing different concentration levels of iron ions at -3 V, room temperature and pH=3.5 for 600 second. Fig. 1 shows the influence of iron concentrations on the deposit composition. The percentage of Fe in a given deposit is lower than its percentages in the bath. A bath solution with high iron content produced an alloy

deposit with low iron content indicating the preferential deposition of less noble zinc leading to anomalous codeposition. This behaviour is attributed to the formation of Zn(OH)₂ film on the cathode surface because of the rise in pH around the cathode film while H₂ evolution occurs [17]. This film suppresses the rate of deposition of iron.

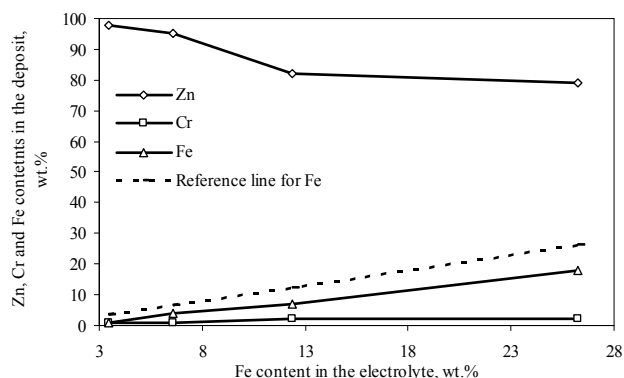


Fig. 1. Influence of iron concentrations on the deposit composition.

Fig. 2 compare the voltammetric response obtained from Cr(III)-free solution, and from Zn(II)+Cr(III)+Fe(III) solutions on steel substrate. Voltammetric results for the Zn-Cr-Fe alloy deposition indicated that the presence of chromium in solution increased the iron deposition and inhibited the zinc deposition processes, since the potential necessary to begin the Zn-Cr-Fe alloy deposition shifted to more positive values. On the reverse scan, only zinc oxidation peaks appeared.

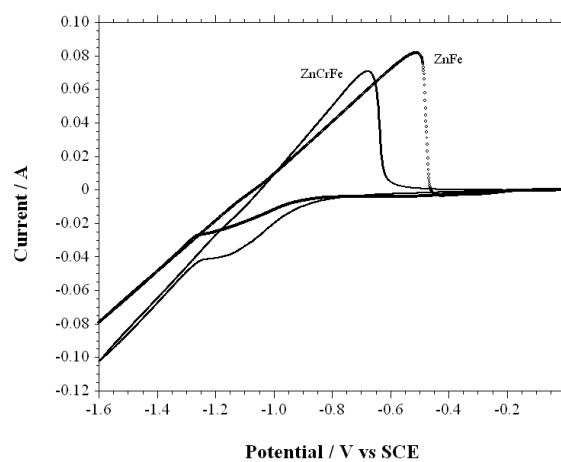


Fig. 2. Cyclic voltammograms for AISI 4140 steel electrode: (a) ZnCl₂ 67.5 g l⁻¹, CrCl₃·6H₂O 159 g l⁻¹, N₂HCH₂COOH 200 g l⁻¹, H₃BO₃ 31.5 g l⁻¹, NH₄Cl 95.4 g l⁻¹, FeCl₃ 16.1 g l⁻¹; (b) ZnCl₂ 67.5 g l⁻¹, N₂HCH₂COOH 200 g l⁻¹, H₃BO₃ 31.5 g l⁻¹, NH₄Cl 95.4 g l⁻¹, FeCl₃ 16.1 g l⁻¹ (pH = 3.5, potential scan rate 10 mV s⁻¹, room temperature).

The XRD patterns of the electrodeposited Zn-Cr and Zn-Cr-Fe films are given in Fig. 3. It is clearly seen that Zn-Cr-Fe alloys have only the η reflection. Adding Cr atoms in the zinc-iron alloy shifted towards to more big reflection angles for all the η phases. The strongest (101)

reflection was observed at Zn-Fe film. A decrease of (101) peak was observed when iron level in the film was increased. The decrease of this peak may be attributed to the decrease of the zinc content in the coating. No Cr phase was observed.

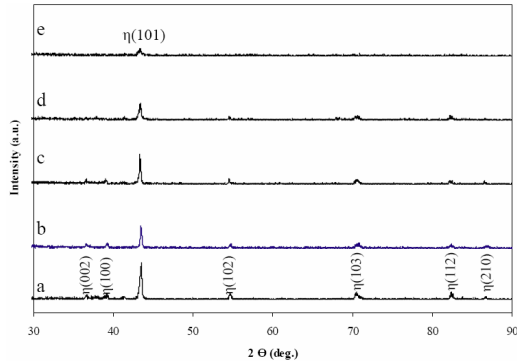


Fig. 3. X-ray diffraction pattern of (a) $Zn_{98}Fe_2$ coating, (b) $Zn_{98}Cr_1Fe_1$ coating, (c) $Zn_{95}Cr_1Fe_4$ coating, (d) $Zn_{91}Cr_2Fe_7$ coating, (e) $Zn_{80}Cr_2Fe_{18}$ coating.

Fig.4 shows the SEM images of Zn-Fe and Zn-Cr-Fe alloy electrodeposits. It is observed that the deposits are generally composed of fine grains. This could be attributed to a large polarization that accompany the deposition process. Large polarization promotes the nucleation rate over the growth rate [18]. The zinc crystals exhibited a range of sizes, and the larger grains were approximately $8\mu m$ diameter on which smaller crystals grew. The morphological structure of the $Zn_{98}Fe_2$ and $Zn_{98}Cr_1Fe_1$ coatings were almost same. The metallic luster and the brightness of the deposit increased with the increasing of the iron content. In the presence of 7 % iron in the film, an appreciable change was observed in the deposit morphology with the grain size decreasing to around $1.5\mu m$ diameter. For the deposits containing 7 and 18 % Ni, a deposit with even smaller grain size was observed. The presence of more iron in the zinc-iron film apparently modified the growth of zinc nuclei, leading to the fine-grained deposits.

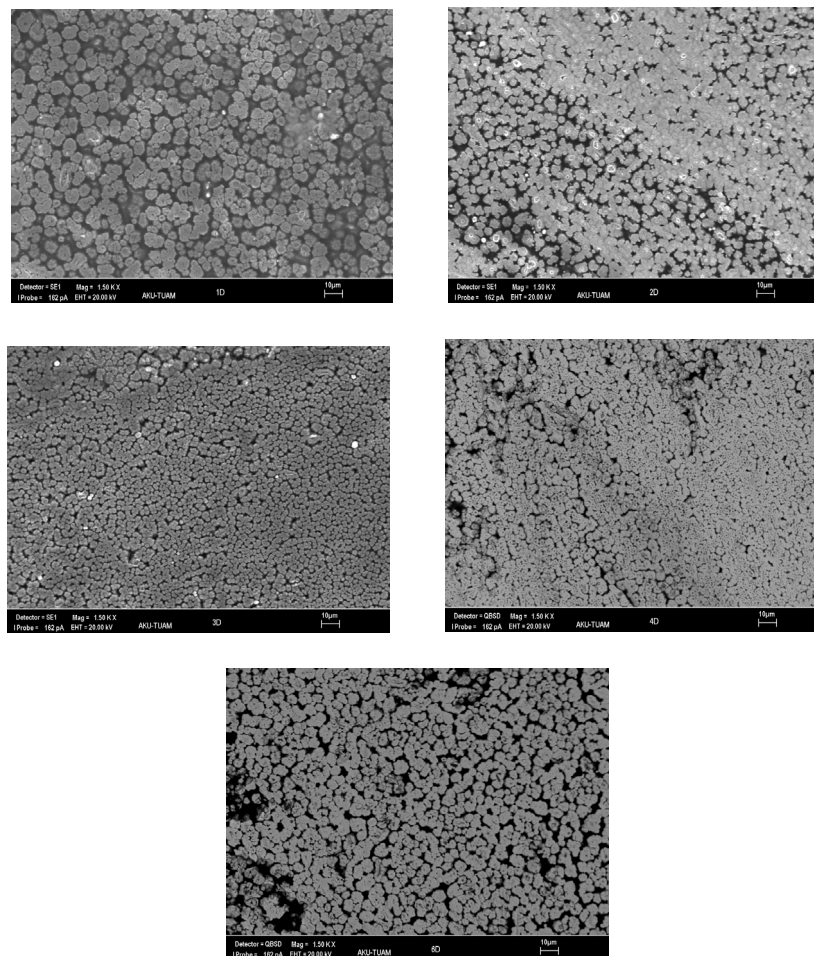


Fig. 4. SEM images of Zn-Fe and Zn-Cr-Fe alloy electrodeposits.

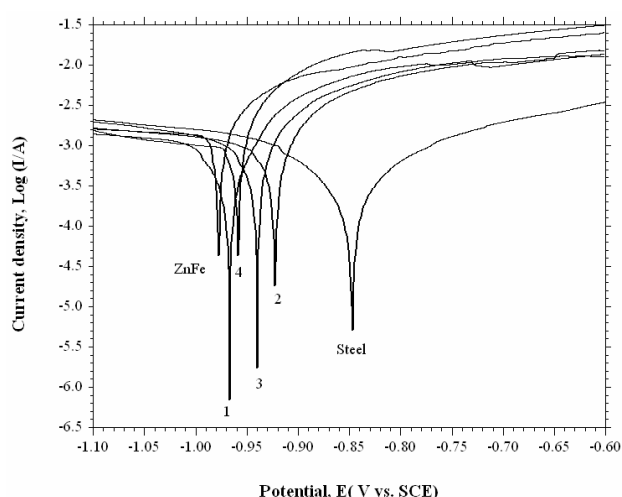


Fig. 5. Corrosion behaviours of electrodeposited Zn-Cr-Fe and Zn-Fe alloys on AISI 4140 substrates.

Fig. 5 shows the corrosion property of Zn-Fe and Zn-Cr-Fe alloys in a 3 wt. % NaCl aqueous solution. The variation in current density with potential is shown in this figure. For comparison, polarization curve of AISI 4140 steel is also shown together. The cathodic polarization curves of all the samples indicated a similar behaviour. However, a difference is evident in anodic polarization behaviour. As can be seen in the figure, biggest decrease in the anodic current density was observed in the coating containing Fe at 4 %. The corrosion potential (E_{corr}) of the smallest corrosive at $\text{Zn}_{98}\text{Cr}_1\text{Fe}_1$ coating and the biggest corrosion resistive coating $\text{Zn}_{95}\text{Cr}_1\text{Fe}_4$ alloy are -0.967 VSCE and -0.922 VSCE, respectively. All ZnCrFe alloys were showed more corrosion resistive behaviour than the Zn-Fe coating. Increase of iron content up to 4 wt. % reduced the reactivity of the zinc alloys and, thereby, ZnCrFe alloys presented a lower degree of corrosion. The increase of iron content in the deposits is caused a finer grain size and an increase in corrosion resistance of Zn-Cr-Fe alloys. It can be seen that the free corrosion potentials of all the zinc alloys more positive but a little negative than that of AISI 4140 steel substrate, which indicates that the Zn-Cr-Fe coating is an ideal anodic protective coating for cobalt or steel products, and can provide longer protection for iron or steel products than pure zinc coatings due to the smaller free corrosion potential difference between the Zn-Cr-Fe coating and that of iron-base substrate.

4. Conclusions

From this study on the effect of alloy composition on the structural, morphological and corrosion properties of Zn-Fe-Cr alloys the following conclusions were drawn:

1. The electroplating of ternary Zn-Cr-Fe alloy showed the phenomenon of anomalous type deposition.

2. Zn-Cr-Fe alloy coatings have the same structure as Zn-Fe alloy.

3. The corrosion rate of Zn-Cr-Fe alloy layer was lower than that of Zn-Fe alloys.

4. The ternary Zn-Cr-Fe deposits showed bright and fine grain sizes.

5. The increase in corrosion resistance of Zn-Cr-Fe deposits can be attributed to the presence of zinc corrosion products.

References

- [1] D. W. Baudrand, A. K. Div, W. Corp, M. Park, *Metal Finish* **33**, 1991.
- [2] C. U. Chisholm, M. El-Sharif, A. Watson, *Trans.Inst.Metal Finish.* **66**, 34 (1988).
- [3] ASM Handbook Volume: 5, Surface Engineering, 595.
- [4] İ. H. Karahan, *J. Mater. Sci.* **24**, 10160 (2007).
- [5] C. J. Lan, W. Y. Liu, S. T. Ke, T. S. Chin, *Surface & Coatings Technology* **201**, 3103 (2006).
- [6] Z. N. Yang, Z. Zhang, J. Q. Zhang, *Surface & Coatings Technology* **200**, 4810 (2006).
- [7] A. P. Yadav, H. Katayama, K. Noda, H. Masuda, A. Nishikata, T. Tsuru, *Corrosion Science* **49**, 3716 (2007).
- [8] C. Q. Yang, Y. C. Zhou, Z. L. Long, *J.of Materials Science Letters* **21**, 1677 (2002).
- [9] M. El-Sharif, X. Wang, C. U. Chisholm, A. Watson, A. Verts and E. Kuzmann *Mater. Sci. Forum* **633**, 163 (1994).
- [10] M. El-Sharif, J. McDougall and C.U. Chisholm *Trans. Inst. Met. Finish.* **77** 4 (1999)139.
- [11] E. W. Brooman In: *Metals Handbook*, ASM, Ohio, 270 (1994).
- [12] T. Pearson, E. Long, *Trans. IMF* **76**(6), B83 (1998).
- [13] A. G. Dolati, M. Ghorbani, A. Afshar *Surf. Coat. Technol.* **166**, 105 (2003).
- [14] C. L. Mcbee, M. Kruger. *Electrochim. Acta* **17**, 1337 (1972).
- [15] R. Tsai, S. Wu, *J. Electrochem. Soc.* **137**, 3057(1990)
- [16] F. Wang, T. Watanabe, *Materials Science and Engineering A* **349**, 183 (2003).
- [17] K. Higashi, H. Fukushima, T. Urakawa, T. Adaniya, K. Matsudo, *J. Electrochem. Soc.* **128**, 2081 (1981).
- [18] E. Gomez, E. Valles, *Bull. Electrochem.* **10**(11-12), 477 (1994).

*Corresponding author: ihkarahan@gmail.com